Simulation of Droplet Impingement on a Solid Surface by the Level Set Method

Junling Hu*[1], Ruoxu Jia[1], Kai-tak Wan[2], Xingguo Xiong[3]
[1]Department of Mechanical Engineering, University of Bridgeport, Bridgeport, CT 06604 USA
[2]Department of Mechanical Engineering, Northeastern University, Boston, MA 02115 USA
[3]Department of Electrical and Computer Engineering, University of Bridgeport, Bridgeport, CT 06604 USA
*jjhu@bridgeport.edu

Abstract: This paper studied the dynamic behavior of a glycerin droplet impinging onto a dry solid substrate using the conservative Level Set method in COMSOL. The droplet impingement process was presented to show the droplet shape and velocity field evolution during the spreading and recoiling of glycerin on a glass surface and a wax surface. The spreading processes on the two surfaces with different surface wettability are similar, but the recoiling processes are different. The spreading factor and apex height evolution of glycerin spreading on a wax surface were compared with the experimental results and good agreements were found. A thorough study of Level Set parameters was also conducted to see their effects on the results.

Keywords: Droplet impingement, level set method, wettability, multiphase flow

1. Introduction

The dynamic behavior of droplet impingement on a solid surface is important to many engineering applications, such as rain drops on automobile windshields, inkjet deposition and metal deposition in manufacturing processes, spray cooling of electronics, and spray coating for various applications. The droplet can spread, splash, and rebound after hitting a solid surface. The resulting phenomena and the final shape of the droplet on a surface depend on several parameters, including the properties of droplet and the impacted surface, the droplet impact velocity, the droplet size, the angle of attack to the surface, the droplet physical properties, the surface wettability, and surrounding pressure [1].

Significant research has been dedicated to study the droplet impingement under various conditions, experimentally, numerically, and analytically [2]. Sikalo and Ganic [2] and Sikalo et al. [3] conducted experiments to study droplet impact of three different fluids on various surface conditions, including dry and wet surfaces, smooth and rough surfaces, hydrophilic and hydrophobic surfaces, and horizontal and inclined surfaces. Tanaka et al. [4] numerically investigated the droplet impact using a two dimensional (2D) lattice Boltzmann method (LBM). Gupta and Kumar [1] developed a 3D LBM model to simulate the spreading behavior of a droplet colliding with a solid dry surface at low impact velocity. Zhou et al. [5,6] studied the shape evolution of micro droplets impingement dynamics in ink-jet manufacturing with both COMSOL phase field method and LBM method.

The dynamic process of droplet impingement is complex and the mechanism of droplet and surface interaction is not fully understood. This paper is aimed to study the dynamic behavior of droplet impinging onto a dry solid surface with different surface wettability using COMSOL Level Set method. As the accurate simulation of droplet impingement is computationally expensive, this project is also aimed to evaluate the numerical tools of COMSOL to simulate droplet impingement process in terms of accuracy and computational cost. We hope to find a set of parameters for a reasonable accuracy at an afford cost. The established droplet impingement model will be further coupled with heat transfer and phase change models for laser metal deposition application.

2. Numerical Modeling

2.1 Governing Equations for Fluid Flow

The fluid flow is incompressible and laminar. Constant density and viscosity are used for both air and liquid droplet. The governing equations for the fluid flow describing the impingement process are time-dependent incompressible Navier-Stokes equations for conservation of mass and momentum formulated as follows:

$$\nabla \mathbf{u} = 0$$

$$\rho\left(\frac{\partial \mathbf{u}}{\partial t} + \mathbf{u}\nabla\mathbf{u}\right) = \nabla\left[-p\mathbf{I} + \mu\nabla\mathbf{u} + (\nabla\mathbf{u})^T\right] + \rho\mathbf{g} + \mathbf{F}_{st}$$

where ρ is the fluid density, **u** is the velocity vector, μ is the fluid dynamic viscosity, t is time, p is fluid pressure, **g** is the gravitational acceleration, $\mathbf{F_{st}}$ is the surface tension force and **I** is the identity matrix.

The interface between the liquid droplet and air and the interface between the liquid droplet and solid substrate are tracked using the conservative Level Set method.

2.2 Conservative Level Set Method

The Level Set method is an Eulerian approach to track the interface for multiphase flow problems on a fixed grid. This paper used a conservative Level Set Method formulated by Olsson and Kreiss [7]. A brief description of this method is given below.

The interface in a Level Set method is captured by a level set function represented by a smeared Heaviside function. The level function changes smoothly across the interface from 0 to 1, where ϕ equals 0 in air and 1 in liquid and the interface is defined by the 0.5 isocontour of ϕ. The interface moves with the fluid velocity, **u**, at the interface. The following equation describes the convection of the reinitialized level set function:

$$\rho\left(\frac{\partial \phi}{\partial t} + \nabla(\phi\mathbf{u})\right) = \gamma\left[\varepsilon\nabla\cdot\nabla\phi - \nabla\cdot\left(\phi(1-\phi)\frac{\nabla\phi}{|\nabla\phi|}\right)\right]$$

where ε is a parameter to determine the thickness of the transition layer and is to be taken as half size of the typical mesh size in the region passed by the droplet. The parameter γ determines the amount of reinitialization of stabilization and must be carefully tuned for each specific problem. If γ is too small, the thickness of the interface might not remain constant and oscillation in ϕ could appear because of numerical instabilities. On the other hand, a too large γ can result in an incorrect interface. A suitable value for γ is the maximum magnitude occurring in the velocity field.

The level set function is used to smooth the density and viscosity jumps across the interface through the definitions

$$\rho = \rho_a + (\rho_l - \rho_a)\phi$$

$$\mu = \mu_a + (\mu_l - \mu_a)\phi$$

where ρ_a, ρ_l, and μ_a, μ_l are the densities and dynamic viscosities of the air and liquid, respectively.

The surface tension force is computed as

$$\mathbf{F}_{st} = \nabla\mathbf{T} = \nabla\cdot\left[\left(\sigma\left(\mathbf{I} - \mathbf{nn}^T\right)\right)\delta\right]$$

where **I** is the identity matrix, **n** is the interface normal, and σ is the surface tension, and δ is the Dirac delta function that is nonzero only at the fluid interface. The interface normal is calculated as

$$\mathbf{n} = \frac{\nabla\phi}{|\nabla\phi|}$$

The delta function is approximated by a smooth function defined by

$$\delta = 6|\phi(1-\phi)||\nabla\phi|$$

2.3 Dimensionless Numbers

The previous studies [3] have shown that the relevant dimensionless numbers that govern droplet-wall interactions are Reynolds number ($Re = \rho u D/\mu$), Weber number ($We = \rho u^2 D/\sigma$), and parameters for surface conditions. The rearrangement of Reynolds number and Weber number gives the Ohnesorge number ($Oh = (We)^{1/2}/Re$). According to Shiaffino and Sonin [6,8], the droplet impact behavior can be classified into four regimes characterized by Weber number as a driving force and Ohnesorge number as a resisting force as shown in Figure 1.

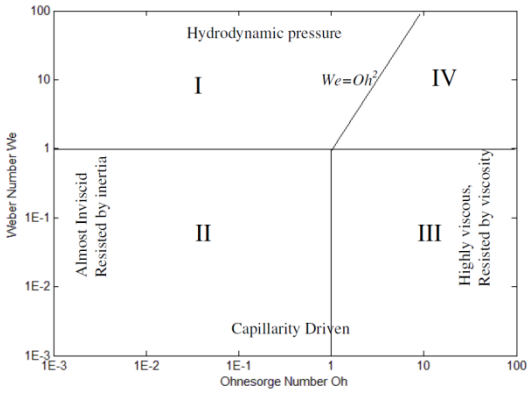

Figure 1. Regime map of spreading [6,8]

3. Numerical model

The numerical model is implemented in COMSOL 4.3b using the Laminar Flow Two-Phase Flow, Level Set interface. The

computational domain of the two-dimensional axis-symmetric problem is shown in Figure 2, where the droplet is placed at a location above the substrate with an initial velocity. The location and initial velocity will ensure an impact velocity of U.

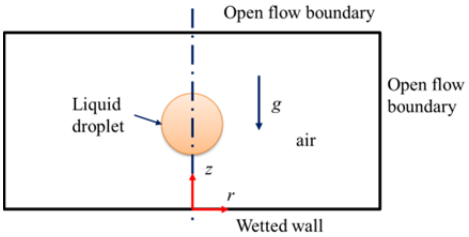

Figure 2. Schematic of computational domain

Open boundary conditions are used at the top and side to simulate an infinite domain. A wetted wall boundary condition is used for the substrate at the bottom. It sets the velocity component normal to the wall to zero and adds a frictional boundary force

$$\mathbf{un}_{wall} = 0$$

$$\mathbf{F}_{fr} = -\frac{\eta}{\beta}\mathbf{u}$$

where η is the fluid viscosity and β is the slip length. The slip length is taken as the default setting of the mesh size. The boundary condition also allows specifying the contact angle θ between the wall and the fluid interface. As shown in Figure 3, contact angle θ affects the droplet wet diameter d and height h during the droplet spreading process.

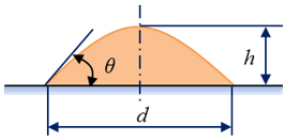

Figure 3. Schematic of droplet attached to a surface: θ, contact angle; h, droplet height; d, droplet wet diameter

4. Results

The paper presented simulation results of a glycerin droplet impinges onto a dry substrate. The simulation condition followed the experimental conditions of Sikalo and Ganic [2] and Sikalo et al. [3]. The diameter of the glycerin droplet is 2.45 mm and the impact velocity is 1.41 m/s. The wettability of the surfaces is represented by static contact angle. Two contact angles are used for the wettability of glycerin on two surfaces, 15° and 94°, for the respective smooth glass and smooth wax substrates. The material properties of glycerin droplet and air are listed in Table 1. The Reynolds number, Weber number, and Ohnesorge number are calculated to be 36.3, 93.8, and 0.267, respectively. The droplet impact behavior is in the regime of hydrodynamic pressure controlled flow.

Table 1. Properties of liquid and air

Parameter	Symbol	Value	unit
Density of glycerin	ρ_l	1220	kg/m^3
Dynamics viscosity of glycerin	μ_l	0.116	Pa·s
Density of air	ρ_a	1.204	kg/m^3
Dynamics viscosity of air	μ_a	1.814×10^{-5}	Pa·s
Surface tension	σ	0.063	N/m

4.1 Droplet Impingement Process

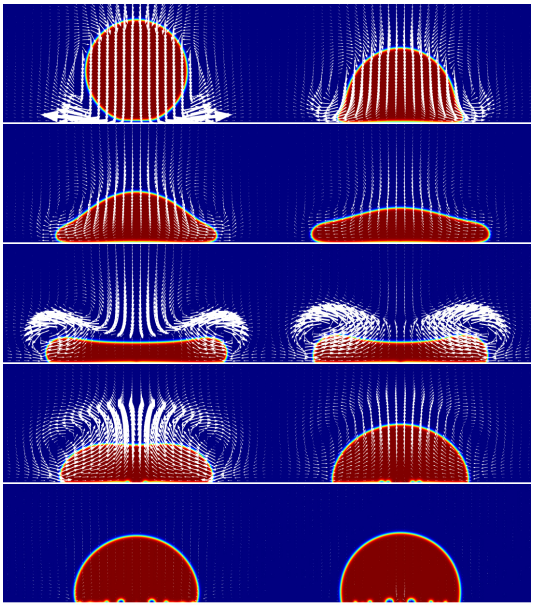

Figure 4. Impingement process of glycerin onto wax surface ($\theta = 94^o$): t = 0.18, 0.68, 1.18, 1.68, 3.38, 4.2, 7.2 10.2, 15.2 and 20 ms; the velocities shown have a scale of 3e-4 before 33.8 ms and 3e-3 thereafter.

A sequence of droplet shape evolution at various time instants are shown in Figure 4 for the dynamic impingement process of a glycerin droplet onto a wax surface. Velocity vectors are overlaid on the droplet volume fraction contours. It can be seen that the spreading process is driven

by the impact pressure and resisted by inertia. The spreading decelerates under the resistance of viscous and capillary forces. The droplet reaches its maximum spreading radius around 3.3 ms and started to recoil under the influence of hydrostatic force and capillary force. No oscillation is observed due to the high viscosity of glycerin.

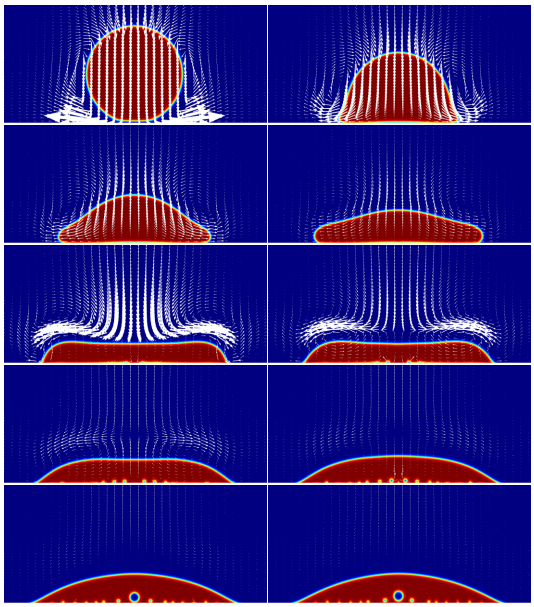

Figure 5. Impingement process of glycerin onto glass ($\theta = 15^o$):: t = 0.18, 0.68, 1.18, 1.68, 3.38, 4.2, 7.2, 10, 15 and 20 ms; the velocities shown have a scale of 3e-4 before 33.8 ms and 3e-3 thereafter.

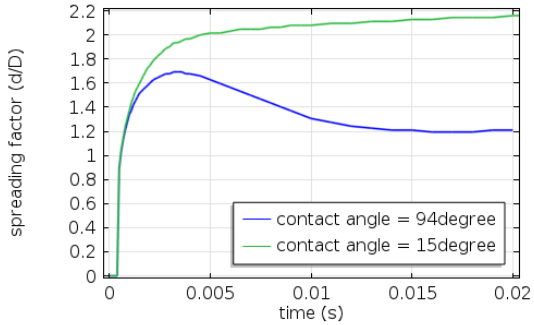

Figure 6. Spreading factor evolution for glycerin impinging onto wax and glass surfaces of corresponding contact angles of 94° and 15°

A similar sequence of droplet impingement process is shown in Figure 5 for a glycerin droplet impinging on to a smooth glass surface. It can be found that the initial spreading process is similar to that on a wax surface because of the dominance of dynamic pressure at the beginning stage of spreading. After the dynamic pressure driving spreading dies down and recoil starts at the droplet top surface, spreading driven by the capillary force starts to take effect and continues through the entire spreading process. The evolution of dimensionless droplet wet diameter (spreading factor $\beta = d/D$) and droplet height (droplet height ratio h/D) are drawn in Figures 6 and 7, respectively.

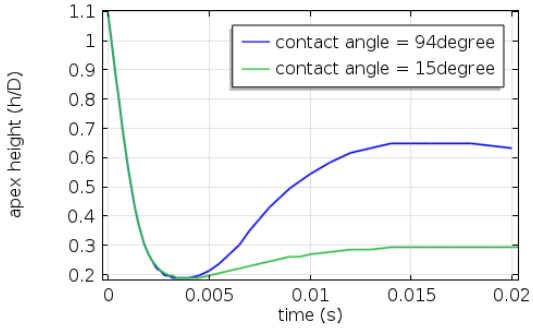

Figure 7. Height to diameter ratio evolution for glycerin impinging onto wax and glass surfaces of corresponding contact angles of 94° and 15°

4.2 Mesh Convergence and Experimental Validation

Two sets of unstructured mesh are used to check mesh convergence. There are 40215 degrees of freedom (DOF) in the set of mesh with a minimum mesh size of 80 μm and 141906 DOF in the one with a 40 μm minimum mesh size. The corresponding running times are 25 min and 1 hour and 32 min on a laptop with Intel core i7 processors and 8 GB RAM. As the density and viscosity of air are much smaller than those of glycerin, the flow in the air is completely driven by the flow in the droplet and does not have much effect on the flow in the droplet, air flow is only found around the droplet. Therefore, the sizes of computational domain have no significant influence on the results and there is no need to provide big air domain to represent an infinite domain.

The spreading factor and dimensionless height calculated with the two meshes are plotted respectively in Figures 8 and 9 and validated by experimental results [3]. It can be seen that even the coarse mesh can predict very good results, especially at the spreading stage. The maximum

spreading factors obtained with the coarse and fine meshes are 1.77, and 1.69, respectively. Comparing with the experimental result of 1.69, the corresponding error ar 4.7% and 0%. The corresponding final equilibrium spreading factors are found to be 1.23 and 1.21 and the errors are 3.9% and 5.5% compared with the experimental result of 1.28. The experiments also show a longer spreading stage than the simulation results. Part of the error is due to the handle of contact angle in the simulation. The static contact angle measured by experiments during advancing and receding are different, and their respective values are $\theta_{adv} = 97^o$ and $\theta_{ret} = 90^o$. A constant contact angle of $\theta = 94^o$ is set as the average of the two angles in the simulation.

The results shown in this paper are calculated with the fine mesh.

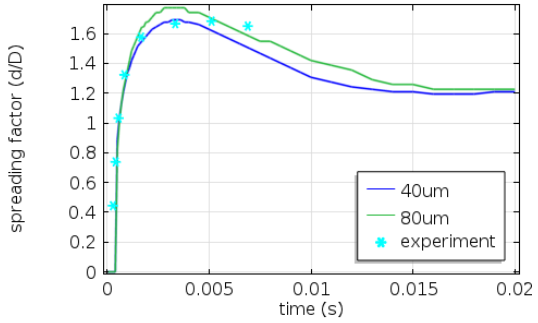

Figure 8. Spreading factor evolution for glycerin impinging onto wax surface ($\theta = 94^o$)

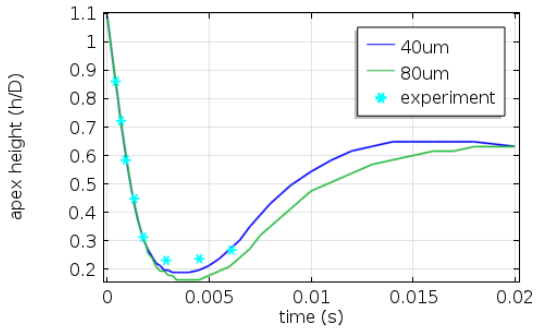

Figure 9. Height to diameter ratio evolution for glycerin impinging onto wax surface ($\theta = 94^o$)

4.3 Parameters for Level Set Method

The simulation results are affected by the Level Set parameters controlling reinitialization and interface thickness, and the choice of conservative form and non-conservative form.

4.3.1 Parameter for Reinitialization

The reinitialization parameter, γ, is recommended to be taken as the maximum velocity in the fluid. Figure 10 shows the the maximum velocity components vary significantly during the dynamic spreading and recoiling process. The velocity is high at the initial impact stage. The reinitialization parameter that is good for the beginning stage would be too high for the entire process. Therefore, a piecewise function, $pw1(t)$, shown in Figure 10 is defined to represent the dynamic maximum velocity. Three cases are run with γ set as $pw1(t)$ and two constants 1.5 and 2 and their results are compared in Figure 11. It can be seen that the results are not very sensitive to γ, especially in the spreading process.

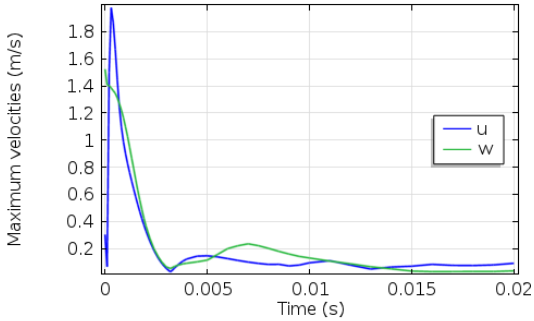

Figure 10. Maximum velocities in the liquid droplets during glycerin impinging onto a wax surface ($\theta = 94^o$)

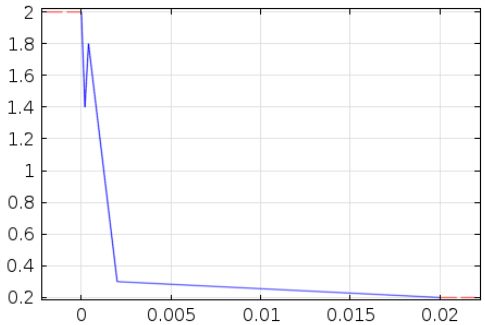

Figure 11. A piecewise function, $pw1(t)$, set for the parameter for reinitialization

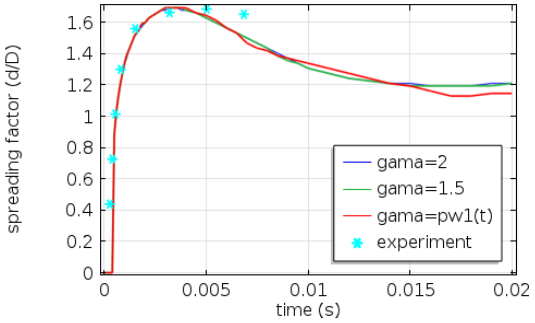

Figure 12. Spreading factor obtained with different γ for glycerin impinging onto a wax surface ($\theta = 94^{o}$)

4.3.2 Parameter Controlling Interface Thickness

The prameter controlling interface, ε_{ls}, is recommended by COMSOL to be taken as be taken as half size of the typical mesh size (h) in the region passed by the droplet.

Two sets of meshes shown in Figure 13 are used to study the effect of ε_{ls} on results. The first set of mesh has a maximum mesh size targeted to be 40 μm in the region passed by the droplet and the second mesh refines the region near the wall. Two simulations are run on the first mesh with $\varepsilon_{ls} = 0.5h$ and $\varepsilon_{ls} = 0.75h$. A third simulaton is run on the second mesh with $\varepsilon_{ls} = 0.75h$. Figure 14 shows the spreading factor obtained with these three simulations and shows a uniform mesh in the droplet region would give the best result. The droplet sectional shape shown in Figure 14 shows the smaller interface thickness gives a sharper interface.

Air bubbles appearing in Figures 4, 5, and 14 are found to be entrained during the spreading and the recoiling process. As air bubbles are not found in the published results [1-6], the formation of air porosity was orignally considered as a result of numerical errors caused by inappropriate level set parameters. It motivated us to conduct a thourough study of level set parameters on the bubble formation. Variations of level set parameters are found not affecting the formation of air bubbles as long as the interface is sharp enough and the mesh is fine enough to resolve the air bubbles.

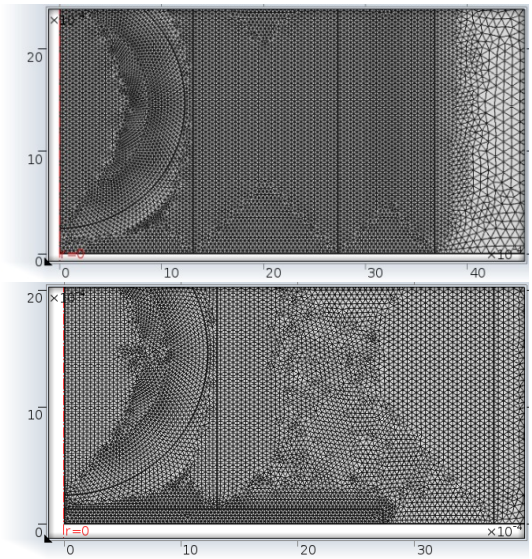

Figure 13. Two sets of meshes used to study the effect of ε_{ls}

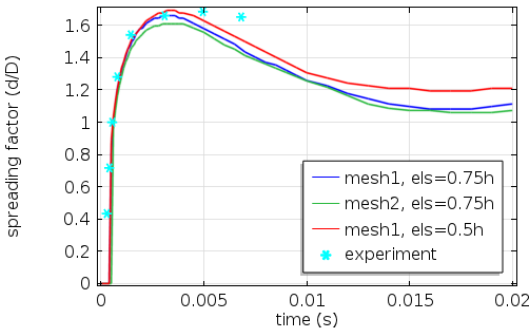

Figure 14. Comparison of spreading factor obtained with different meshes and parameters controlling interface thickness ε_{ls}

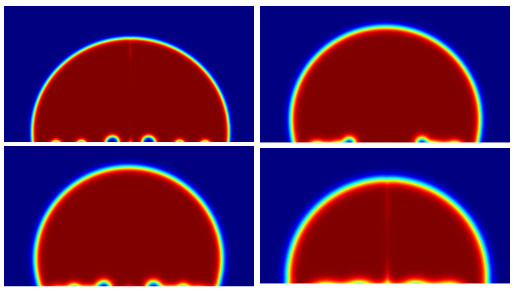

Figure 15. Droplet sectional shape at t = 0.2 obtained by: (a) mesh1 and $\varepsilon_{ls} = 0.5h$, (b) mesh1 and $\varepsilon_{ls} = 0.75h$, (c) mesh2 and $\varepsilon_{ls} = 0.75h$(d) minimum mesh size of 80 μm and $\varepsilon_{ls} = 0.5h$

4.3.3 Conservative and Nonconservative Level Set

Compared to conservative Level Set form, Non-conservative Level Set is easier to converge, but has a loss or gain of mass due to numerical diffusion. As seen in Figure 16, droplet mass is conserved with the conservative Level Set. The mass gain and loss with the nonconservative Level Set in this study is below 1%, far below the acceptable range of 3%. The simulation results obtained with both methods are close, as seen in the droplet spreading factors shown in Figure 17.

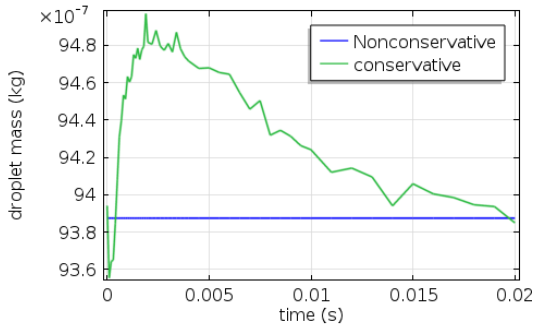

Figure 16. Comparison of droplet mass with conservative Level Set and non-conservative Level Set

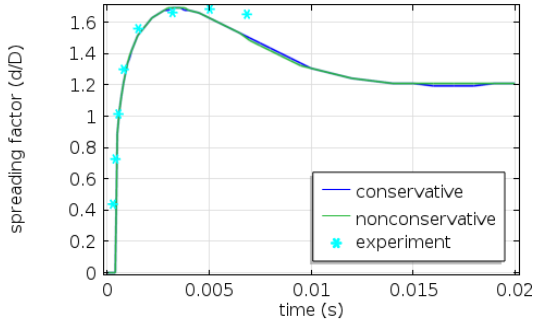

Figure 17. Comparison of spreading factors obtained by conservative Level Set and non-conservative Level Set

5. Conclusions

This paper simulated the dynamic process of glycerin impinging onto two substrates with different wettability using the conservative Level Set method. The dynamic process was validated against experimental results. It was found that the Level Set method can predict the overall dynamic process very well, especially the spreading process. Level set parameters are also studied to see their effects on the spreading factor and the porosity formation. Level set parameters need to be tuned for convergence and accuracy, but they are also in a wide enough range for easy set up. Nonconservative level set method can also be used in the simulation of droplet impingement of glycerin with good accuracy.

6. References

1. Amit Gupta and Ranganathan Kumar, Droplet impingement and breakup on a dry surface, *Computers and Fluids*, **39**, 1696-1703 (2010).
2. S. Sikalo and E.N. Ganic, Phenomena of droplet-surface interactions, *Experimental Thermal and Fluid Science*, **31**, 97-110 (2006).
3. S. Sikalo, M. Marengo, C. Tropea, and E.N. Ganic, Analysis of impact of droplets on horizontal surfaces, *Experimental Thermal and Fluid Science*, **25**, 503-510 (2002).
4. Y. Tanaka, Y. Waashio, M. Yoshino, and T. Hirata, Numerical simulation of dynamic behavior of droplet on solid surface by the two-phase lattice Boltzmann method, *Computers and Fluids*, **40**, 68-78 (2011).
5. W. Zhou, D. Loney, A. G. Fedorov, F. L Degertekin, D. W. Rosen, Impact of polyurethane droplets on a rigid surface for ink-jet printing manufacturing, *21st Solid Freeform Fabrication Symposium*, 2010, Austin, TX.
6. W. Zhou, D. Loney, A. G. Fedorov, F. L Degertekin, D. W. Rosen, Shape evolution of droplet impingement dynamics in ink-jet manufacturing, *22nd Solid Freeform Fabrication Symposium*, Aug.8-10, 2011, Austin, TX.
7. E. Olsson and G. Kreiss, A conservative level set method for two phase flow, *J. of Comp. Phys.*, **210**, 225-246 (2005)
8. S. Shiaffino and A.A. Sonin, Molten droplet deposition and solidification at low Weber numbers, *Phys. Fluids*, **9**, 3172-3187 (1997)